

Hydrostatic equilibrium conditions in the galactic halo

P.M.W. Kalberla and J. Kerp

Radioastronomisches Institut der Universität Bonn, Auf dem Hügel 71, D-53121 Bonn, Germany

Received 19 March 1998 / Accepted 25 August 1998

Abstract. The large scale distributions of gas, magnetic field and cosmic rays in the galactic halo are investigated. Our model is based on the analysis of all-sky surveys of H I gas (Leiden/Dwingeloo survey), soft X-ray radiation (*ROSAT* all-sky survey), high energy γ -ray emission (*EGRET* > 100 MeV), and radio-continuum emission (408 MHz survey).

We found a stable hydrostatic equilibrium configuration of the Galaxy which, on large scales, is consistent with the observations. Instabilities due to local pressure or temperature fluctuations can evolve only beyond a scale height of 4 kpc. We have to distinguish 3 domains, with different physical properties and scale heights:

1) The gaseous halo has an exponential scale height $h_z \simeq 4.4$ kpc. Its radial distribution is characterised by a galactocentric scale length $A_1 \simeq 15$ kpc. On large scales all components of the halo – gas, magnetic fields and cosmic rays – are in pressure equilibrium. The global magnetic field is regularly ordered and oriented parallel to the galactic plane.

2) The disk has a vertical scale height of about 0.4 kpc. Characteristic for this region is the high gas pressure. The associated magnetic field is irregularly ordered and its equivalent pressure is only $\simeq 1/3$ of the gas pressure. The cosmic rays are decoupled from gas and magnetic fields.

3) The diffuse ionised gas layer with a vertical scale height of about 0.95 kpc and a radial scale length of $A_1 \simeq 15$ kpc acts as a disk-halo interface. The magnetic field in this region has properties similar to that in the disk. However, here the cosmic rays are coupled to the magnetic fields in contrast to the situation within the galactic disk. The gas pressure in this transition region is essential for the stability of the galactic halo system.

Applying the model we can derive some major properties of the Milky Way:

Assuming that the distribution of the gas in the halo traces the dark matter, we derive for a flat rotation curve a total mass of $M = 2.8 \cdot 10^{11} M_\odot$. The mass of the galactic halo is $M_{halo} \simeq 2.1 \cdot 10^{11} M_\odot$.

We find that turbulent motions in the gaseous halo can be described by the Kolmogoroff relation. The smallest clouds, which are compatible with such a turbulent flow, are at temperatures close to 3 K. They have linear sizes of ~ 20 au and masses of

$\sim 2 \cdot 10^{-3} M_\odot$. A significant fraction of the galactic dark matter may be in this form.

Key words: Galaxy: halo – Galaxy: kinematics and dynamics – ISM: clouds – cosmic rays – ISM: magnetic fields – dark matter

1. Introduction

Attempts to describe the gaseous galactic halo date 40 years back. At the IAU Symposium No. 8, Pikelner & Shklovsky (1958) presented the first model of a galactic halo composed of gas, magnetic fields and cosmic rays. The assumption of pressure equilibrium between these three components yielded a model of an almost spherical neutral but highly turbulent halo. They proposed that this halo would be detectable in H I 21-cm radiation with a line velocity dispersion of $\simeq 70 \text{ km s}^{-1}$. At that time however, such emission lines could not be observed because of technical constraints.

Spitzer (1956) pointed out, that energy dissipation by shocks must cause a rarefied hot ($T \simeq 10^6$ K) halo. Assuming that this halo plasma is in hydrostatic equilibrium with the gravitational potential of the galactic disk, Spitzer estimated a plasma scale height of $\simeq 8$ kpc and a midplane density of $5 \cdot 10^{-4} \text{ cm}^{-3}$.

Parker (1966) focused his analysis on stability considerations between gas, magnetic fields and cosmic rays in an equilibrium configuration. He found that it is difficult to maintain a stable configuration due to hydromagnetic self-attraction. From this kind of stability considerations it became apparent that they are of major concern for the understanding of equilibrium conditions in the galactic halo.

Lachièze-Rey et al. (1980) included turbulent motions into their stability considerations. This turbulent pressure component mitigated the influence of the “Parker-instabilities” on the hydrostatic equilibrium models and enabled new attempts to find conditions under which a stable equilibrium configuration of the Galaxy could exist.

With respect to the considerations of Lachièze-Rey et al. (1980), Bloemen (1987) proposed an extended high temperature halo. At a vertical distance of $1 < |z| < 3$ kpc the halo gas temperature should be $T \simeq (2 - 3) \cdot 10^5$ K while within the disk and above $|z| > 3$ kpc the temperature should be $T \simeq$

10^6 K. This halo plasma should emit significant amounts of X-ray photons within the 1/4 keV and 3/4 keV energy bands. At this time it was assumed that most of the soft X-ray radiation originates from the local cavity (Snowden et al. 1990).

To reduce the necessity of a halo plasma, Boulares & Cox (1990, hereafter B&C) introduced magnetic-tension forces in their considerations of a galactic hydrostatic equilibrium. B&C pointed out, that a hydrostatic equilibrium necessarily needs high $|z|$ extensions for all components: gas, magnetic fields and cosmic rays. In particular, they deduced that the velocity dispersion of the gaseous component has to increase up to 60 km s^{-1} for a stable hydrostatic equilibrium configuration.

Bloemen (1987) and B&C came to different conclusions concerning the existence of a hot galactic halo plasma. However, there was a general agreement between these papers that it is essential to stabilise the hydrostatic equilibrium configuration by the pressure of the gaseous component. The gaseous halo component - regardless of its physical state - must necessarily be supported by the galactic disk and reach $|z|$ distances of $\simeq 5 \text{ kpc}$.

In the mean time, the observational database increased significantly with respect to the gaseous component. The diffuse ionised hydrogen layer is now an established component of the Galaxy (Reynolds 1997). The *ROSAT* mission established the existence of an X-ray emitting plasma within the galactic halo (Pietz et al. 1998a, 1998b, Wang 1998). The new Leiden/Dwingeloo H I 21-cm drop survey revealed the existence of an H I high-dispersion-velocity component (Westphalen et al. 1997, Kalberla et al. 1997a, 1998). The Goddard-High-Resolution-Spectrograph on board of the *HST* improved our knowledge about the distribution of highly ionised gas above the galactic disk (Savage et al. 1997). Thus, it is of considerable interest to re-investigate the hydrostatic equilibrium considerations including these new data sets.

Of special interest concerning the gaseous components are the following discoveries:

1. H I gas with a velocity dispersion of up to 35 km s^{-1} has been found towards the galactic poles by Kulkarni & Fich (1985). Lockman & Gehman (1991) pointed out, that the turbulent energy of this H I component can support layers up to distances of $|z| > 1 \text{ kpc}$. Westphalen et al. (1997) and Kalberla et al. (1998) analysed the Leiden/Dwingeloo survey (Hartmann, 1994 and Hartmann & Burton, 1997, henceforward LDS) and detected H I gas with a velocity dispersion of $\sigma \simeq 60 \text{ km s}^{-1}$. Kalberla et al. (1997b) investigated quantitatively the disagreement between the LDS and the Bell Laboratories H I survey (BLS, Stark et al. 1992). They came to the conclusion that the velocity dispersion of 35 km s^{-1} derived from the BLS is biased by insufficient corrections of the instrumental baselines. Because of the higher velocity resolution and the larger velocity coverage of -450 km s^{-1} to $+400 \text{ km s}^{-1}$, the instrumental baseline uncertainties of the LDS are significantly less than those of the BLS. Kalberla et al. (1998) constrained the H I velocity dispersion to $\sigma = (60 \pm 3) \text{ km s}^{-1}$ by a reanalysis of the

LDS survey. They proposed that such lines originate from a layer of H I gas, co-rotating with the disk, with a scale height of $h_z = 4.4 \text{ kpc}$.

2. At optical wavelengths Münch & Zirin (1960) first found absorption lines indicating the existence of neutral gas above $|z| \geq 500 \text{ pc}$ (for a review see Danly, 1990). In the mean time absorption line measurements established the existence of highly ionised gas within the galactic halo. In a recent paper, Savage et al. (1997) derived exponential scale heights for different species of ionised atoms: $h_z(\text{SiIV}) = 5.1(\pm 0.7) \text{ kpc}$, $h_z(\text{CIV}) = 4.4(\pm 0.6) \text{ kpc}$ and $h_z(\text{NV}) = 3.9(\pm 1.4) \text{ kpc}$. In a second approach, they focused their attention to the kinematical properties of the gas. A turbulent velocity of $\sigma \simeq 60 \text{ km s}^{-1}$ was derived from CIV lines. The data are consistent with the model that the highly ionised gas co-rotates with the galactic disk. For the CIV absorption profiles they derived a dynamical scale height of $h_z(\text{CIV}) = 4.5(\pm 1.6) \text{ kpc}$. The gas pressure derived from this velocity dispersion is not sufficient to stabilise the gas at scale heights of $h_z = 4.4 \text{ kpc}$. Accordingly, Savage et al. (1997) concluded that additional pressure sources are needed, most probably from magnetic fields and cosmic rays.
3. *ROSAT* observations of the Draco cloud suggested that diffuse soft X-ray emission originates from outside of the local X-ray plasma (Snowden et al. 1991). Up to now it is a matter of debate whether the galactic X-ray halo has a patchy or smooth intensity distribution. In general, we know that the observed diffuse soft X-ray emission is a superposition of the X-ray radiation of the "local hot bubble" (Snowden et al. 1990, 1998), the galactic X-ray halo (Pietz et al. 1998a, Wang 1998) and the extragalactic background radiation (Hasinger et al. 1998). In a recent paper Pietz et al. (1998a) demonstrated that the galactic X-ray halo radiation can be modelled very well by a vertical distribution of a pervasive gas component with $T \simeq 1.5 \cdot 10^6 \text{ K}$ and an exponential scale height of $h_z = 4.4 \text{ kpc}$.

These results, which were derived by different authors from different databases, indicate that there is convincing evidence for a gaseous galactic halo with a vertical scale height of $h_z = 4.4 \text{ kpc}$. To obtain a comprehensive view of the large scale structure of our Galaxy we performed a new analysis following Parker (1966). We investigated quantitatively the distribution of the gas, the magnetic fields and cosmic rays by studying state-of-the-art data sets. We intend to present our entire model and all of its variables right from the beginning. This gives us the possibility to describe the model in the necessary detail. Most of the model parameters cannot be determined independently from one individual database. In practice, one has to recalculate all parameter values if only one is changing, this however cannot be described in a concise way. The following sections describe the procedures which were used to evaluate the parameter values. In Sect. 2 we describe the basic assumptions concerning our hydrostatic model; in Sect. 3 we present the analysed data and the derived parameters. In Sect. 4 we describe the large-scale

galactic distribution of gas. In Sect. 5 we verify the model in comparison with the observed galactic synchrotron and γ -ray emission. In Sect. 6 we discuss the stability of the galactic halo and discuss limits for the galactic origin of high-velocity clouds (HVCs). In Sect. 7 we estimate the dark matter content of the galactic halo. In Sect. 8 we discuss turbulent processes in the halo. In Sect. 9 we summarise and discuss our results.

2. Equilibrium conditions

The ‘‘classical’’ publication of Parker (1966) raised the question whether or not the galactic disk and halo may be in a hydrostatic equilibrium state. In particular the most recent publications in this field by Bloemen (1987) and B&C discuss stability considerations in great detail. In addition, it is important to realize that Lockman & Gehman (1991) generalised the concept of an isothermal equilibrium concept of our Galaxy. The considerations of these papers mark our starting point in investigating the physical conditions within the galactic disk and halo.

2.1. Basics

According to Parker (1966) a hydrostatic equilibrium of an interstellar gas phase against the gravitational acceleration in z direction is described by

$$\frac{d}{dz}(1 + \alpha + \beta) p(z) = -n(z) d\Phi(z)/dz. \quad (1)$$

Where $p(z) = n(z) <v^2>$ denotes the gas pressure with $\sigma_v = \sqrt{\langle v^2 \rangle}$ as the total rms random gas velocity dispersion in the z direction, $p_{\text{mag}}(z) = B^2/(8\pi) = \alpha p(z)$ the magnetic field pressure and $p_{\text{cr}}(z) = \beta p(z)$ the pressure of the cosmic ray component. The total gas density is $n(z)$ and $\Phi(z)$ the galactic gravitational potential at a distance z perpendicular to the galactic plane. Eq. (1) is solved by:

$$n(z) = n_0 \exp\left[\frac{-\Phi(z)}{\langle v^2 \rangle (1 + \alpha + \beta)}\right]. \quad (2)$$

n_0 denotes here the mid-plane density. It is assumed that σ_v , α and β are independent of z , consistent with an isothermal gas approach.

The parameters α and β are of utmost importance here. The total pressure is $(1 + \alpha + \beta) p(z)$. Thus the magnetic fields and cosmic rays are sources of pressure within the galactic interstellar medium.

2.2. Gravity

We use the gravitational potential as derived by Kuijken & Gilmore (1989). This potential satisfies, for large z distances, the asymptotic condition for a flat rotation curve derived by B&C (their Eq. 1). The Kuijken & Gilmore potential does not require significant amounts of hidden disk-mass in the solar neighbourhood. Moreover, Cr ez e (1991) demonstrated that the Kuijken & Gilmore potential is in good agreement with the Bienam e et al. (1987) potential which was used by B&C.

Eq. (2) gives the z dependence of the gas density n only as a function of z . As discussed by de Boer (1990), the gravitational potential depends strongly on the galactocentric distance R . Rather than modifying the potential $\Phi(R, z)$ itself as function of both, R and z , we use the separation approach of Taylor & Cordes (1993, see their discussion in Sect. 3.1) based on squared hyperbolic secants which were first introduced by Spitzer (1942). This modifies Eq. (2) to:

$$n(R, z) = g_1(R) n_0 \exp\left[\frac{-\Phi(z)}{\sigma_v^2 (1 + \alpha + \beta)}\right] \quad (3)$$

where $n_0 = n(R_\odot, 0)$ is the mid-plane density at the radial position of the Sun. The radial term is

$$g_1(R) = \text{sech}^2(R/A_1)/\text{sech}^2(R_\odot/A_1), \quad (4)$$

with $R_\odot = 8.5$ kpc.

3. Data

3.1. The composition of the galactic gas phase

A common result of the investigation of Bloemen (1987) as well as of B&C is, that a high gas pressure is needed to stabilise the galactic halo. To provide this pressure, Bloemen (1987) predicted a hot X-ray emitting plasma within the galactic halo. In contrast to this approach B&C suggested that the necessary high gas pressure can be provided without such a plasma, but by increasing the velocity dispersion of the cooler gas up to $\sigma_v = 60$ km s⁻¹ at high $|z|$ -distances. The datasets now available can set tight constraints to both proposed gas components. This focuses our view onto the gas distribution and its physical condition, as the most important constituent of our considerations.

We intend to describe only the large scale structure of the Galaxy. Accordingly, we exclude the molecular clouds as well as the influence of the galactic spiral structure. This approach is not an oversimplification, because to extract significant information from the observational data one has to average the data across tens of degrees. Accordingly, the area filling factor of the molecular species, especially towards high galactic latitudes (Hartmann et al. 1998) is negligibly small, and so is the influence of the spiral structure, except very close to the galactic plane.

Within the galactic disk the optical depth of the HI reaches unity. Because of the strong photoelectric absorption of the galactic ISM within the plane the ROSAT X-ray data reveal only information about the local environment. Accordingly, we anticipate the largest uncertainties close to the galactic plane ($b \leq 10^\circ$), while towards high latitudes we have the opportunity to make a quantitative analysis of the new observational data of the gaseous phases.

3.2. The galactic halo

3.2.1. Neutral gas in the halo

Kalberla et al. (1998) detected a high-velocity-dispersion component with $\sigma_v = (60 \pm 3)$ km s⁻¹. Several critical inves-

tigations were performed to exclude any instrumental artefact which may mimic such an H I line profile. This high-velocity-dispersion component has a column density $N_{\text{HI}} = 0.14 \cdot 10^{20} \text{ cm}^{-2}$ towards the galactic poles. Henceforward, this component will be abbreviated as Neutral Halo Medium (NHM).

3.2.2. X-ray gas in the halo

Pietz et al. (1998a) cross-correlated the *ROSAT* all-sky survey (Snowden et al., 1995) and the LDS and evaluated the X-ray radiation transport. For the X-ray plasma Pietz et al. (1998a) derived a temperature of $T = 1.5 \cdot 10^6 \text{ K}$, and an emission measure $EM = \int n_e(z)^2 dz = 4.0 \cdot 10^{-3} \text{ pc cm}^{-6}$ towards the galactic poles. To model the detected galactic centre/anti-centre X-ray intensity asymmetry, the radial distribution function g_1 (Eq. 4) according to Taylor & Cordes (1993) was fitted to the data. Pietz et al. (1998a) derived a radial scale length of $A_1 \simeq 15 \text{ kpc}$ and a vertical scale height of $h_{\text{X-ray}} \simeq 4.4 \text{ kpc}$. This X-ray halo plasma will be abbreviated as Hot Halo Medium (HHM).

3.2.3. Highly ionised gas in the halo

Collisionally ionised gas at temperatures $T \simeq 10^5 \text{ K}$ is present within the galactic halo. In a recent paper Savage et al. (1997) determined the scale height for several species and derived on average $h_z \simeq 4.4 \text{ kpc}$. Because of the existence of the galactic halo plasma we do not consider this ionised gas phase as an individual component, but as an intermediate state between the neutral and X-ray gas phase of the galactic halo.

3.3. The disk-halo interface

Towards the galactic plane, the Galaxy hosts the diffuse ionised gas (DIG). This component, frequently called ‘‘Reynolds-Layer’’, will be incorporated in our model. We use the values given by Reynolds (1997), with a column density of $N_{\text{H}\alpha} = 0.65 \cdot 10^{20} \text{ cm}^{-2}$ and a scale height of 0.95 kpc . This scale height is an intermediate one between those of the galactic disk and the halo. The question arises whether this layer may have the properties of the disk or the halo. In all calculations we tried to differentiate between these two alternatives.

3.4. The galactic disk

The interstellar matter in the galactic disk is a superposition of various different gas phases with different scale heights. We found that the gas parameters used by Bloemen (1987), B&C and by Lockman & Gehman (1991) do not represent the observed large scale H I distribution very well. This discrepancy between the modelled and observed H I column density distribution is most probably caused by the presence of the local void of neutral matter, which may have affected previously the determination of gas parameters. Accordingly, the position of the Sun within the Galaxy is not representative for the general interstellar medium. In our approach we optimised the gas parameters by

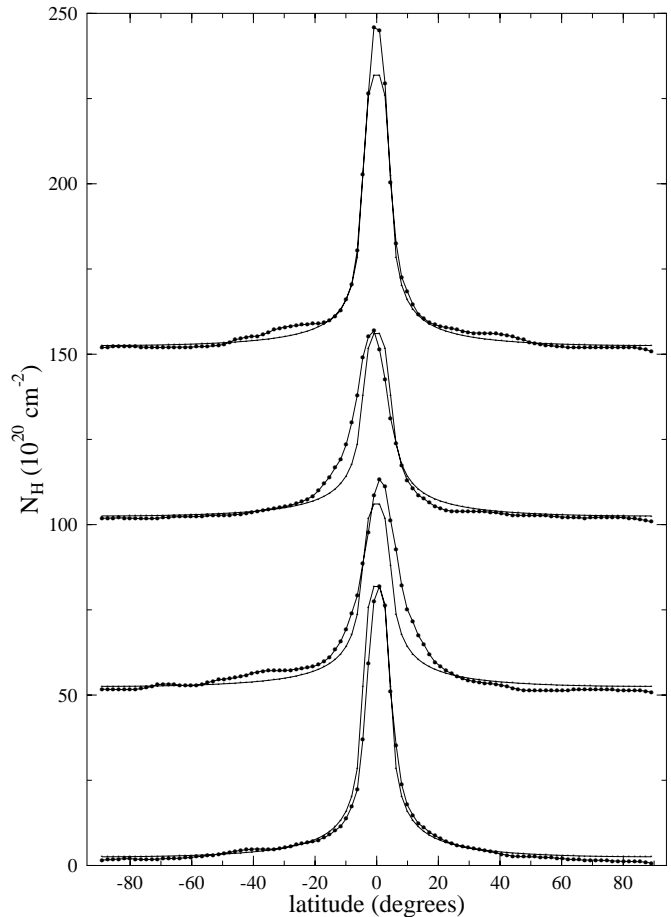


Fig. 1. The averaged H I column density distribution as a function of the galactic latitude for the galactic quadrants 1 to 4 (bottom to top). The observational data are indicated by the connected dots while the modelled H I column density distributions are marked by the solid lines. The modelled distribution accounts for the CNM, WNM and the NHM. The model fits the observational data well. However, a deficiency of neutral atomic gas in the northern galactic hemisphere is visible. Here we see the influence of the local void of neutral matter on the H I column density distribution. Also within the galactic plane $|b| \leq 10^\circ$ some deviations are present. The parameters of the modelled H I column density distribution were used for further calculations.

fitting the overall observed H I column density extracted from the LDS as a function of galactic latitude. The southern gap of the LDS data was filled by the Dickey & Lockman (1990) data. Fig. 1 gives a quantitative comparison between the LDS data (connected dots) and modelled H I gas parameters for the CNM, WNM and NHM (solid line). Our best fit gas parameters are given in Table 1. In comparison with Bloemen (1987) or B&C we restricted our representation to those gas phases which were found to be indispensable. The molecular gas within the galactic plane was included initially in our analysis but omitted after we found that our conclusions were unaffected by this gas phase.

Table 1. The table compiles the best fit parameters of the hydrostatic equilibrium model of our Galaxy. n_0 denotes the volume density of the gaseous phases. σ the velocity dispersion for some gas phases derived from observations. N is the derived column density of the gas phase towards the galactic poles (half the column density across the total disk). h_z is the vertical scale height of each gas component. α denotes the ratio of magnetic field to gas pressure, while β is the ratio of the cosmic ray to gas pressure. Both ratios are determined for the disk, the disk-halo interface and the galactic halo individually, but not for each gaseous component. Accordingly, the values for the CNM and WNM in the disk as well as for the NHM and HHM in the halo are the same.

Component	n_0 [cm ⁻³]	σ [km s ⁻¹]	N [10 ²⁰ cm ⁻²]	h_z [kpc]	α	β
– Disk:						
CNM	0.3	7.5	1.28	0.15	1/3	0
WNM	0.1	17	1.14	0.40	1/3	0
– Disk-halo interface:						
DIG	.024	–	0.65	0.95	1/3	1/3
– Halo:						
NHM	.0012	60	0.15	4.40	1	1
HHM	.0013	–	0.14	4.40	1	1

3.5. Magnetic field and cosmic rays

Observationally the determination of the total magnetic field strength and orientation is affected by considerable uncertainties. The common way for the determination of these quantities is to study the galactic synchrotron emission. As discussed by Ginzburg & Syrovatskii (1964), the synchrotron emission is a tracer for the interaction between the galactic electron component of the cosmic rays and the magnetic fields.

We analysed the 408 MHz survey of galactic radio-continuum emission (Haslam et al., 1982). The major outline of our investigations is based on previous publications by Phillipps et al. (1981a,b) and Beuermann et al. (1985). These latter authors found that the observed galactic synchrotron radiation is a superposition of emission originating from a “galactic thin disk” and a “thick disk”. According to Beuermann et al. (1985), the absolute majority of the detected synchrotron emission (90%) originates from the thick disk, up to z distances of several kpc above the galactic plane. In Sect. 5.1 we re-analysed the 408 MHz synchrotron intensity distribution to investigate the quantitative correlation between our model and the observational data.

The cosmic ray particles interact with gas and photons. As a result, γ -ray emission is produced (for a review see Bloemen, 1989). In combination with the 408 MHz survey data we use the high energy γ -ray emission observed with *EGRET* at energies > 100 MeV (Fichtel et al., 1994) to compare our model with the observational data, discussed in Sect. 5.2.

4. The model

We studied the galactic hydrostatic equilibrium by calculating disk-halo models according to Eq. (3) and compared them with the data sets mentioned before. Our calculations showed, that

the Galaxy can be subdivided into three major regions: the galactic disk, the disk-halo interface and the galactic halo. The gas phase within each individual region has on average no influence on the neighbouring regions. This separation is introduced by our approach of an isothermal hydrostatic equilibrium state of the entire Galaxy on large angular scales. Thus the equilibrium conditions described by the parameters α and β are defined independently for each gas phase in each individual region. Our aim was to find an unique set of parameters in quantitative agreement with all large scale survey data sets under consideration.

The basic parameters (in particular the gas, the magnetic fields and the cosmic rays) of a hydrostatic equilibrium model are *not* independent of each other. Accordingly, a variation of a single model parameter needs to be followed by a re-calculation of all modelled distributions. To be concise, we give the parameters of the best fit model only, but discuss the parameters and their limitations by comparing the observational data with the model in the text below.

4.1. Radial distribution

The radial gas density distribution was derived according to Eq. (4) from the LDS (Kalberla et al. 1998) and *ROSAT* data (Pietz et al. 1998a). Pietz et al. (1998a) derived a best fit value $A_1 = 15^{(+5.0)}_{(-2.5)}$ kpc for the HHM from an analysis of the soft X-ray background data in the *ROSAT* 1/4 keV and 3/4 keV energy band. The same value was found to fit the NHM distribution best (Kalberla et al. 1998). Taylor & Cordes (1993) estimated a radial scale length $A_1 \simeq 20$ kpc for the DIG by analysing pulsar data. Lazio & Cordes (1998) determined A_1 to be 17 kpc from a VLBA survey of extragalactic sources towards the galactic anti-centre. Here we use $A_1 = 15$ kpc which was found to give a satisfactory representation for *all* of the gas components in Table 1, even for CNM and WNM as shown Fig. 1.

According to Dickey & Lockman (1990) there is a deficiency of H I gas at galactocentric radii $R < 4$ kpc. The LDS data confirmed this deficiency. We modelled the radial density decrease in the inner Galaxy by applying a linear scaling function proportional to R multiplied with $g_1(R)$. This linear intensity decrease was applied to $g_1(R)$ within the radial boundary of $4 \text{ kpc} \geq R \geq 0 \text{ kpc}$ resulting in a 40% drop-off at $R = 0$ kpc. This normalised radial density distribution is shown in Fig. 2.

4.2. Vertical distribution

According to Eq. (2), the vertical density distribution of the gas phase is derived in a first step from the H I and X-ray data (Table 1). In Fig. 3 we show the $n(z)$ -distribution of the galactic disk components (CNM and WNM), the disk-halo interface (DIG) and the halo gas phases (NHM and HHM). Fig. 3 represents the vertical density distribution at the galactocentric radius of the Sun ($R_\odot = 8.5$ kpc).

It is well known that the scale height of the H I in the disk increases significantly toward larger galactocentric radii (e.g. Burton, 1988). Such an effect, called galactic flaring, is expected also for the gas in the halo (Ferrière 1998). However, flaring

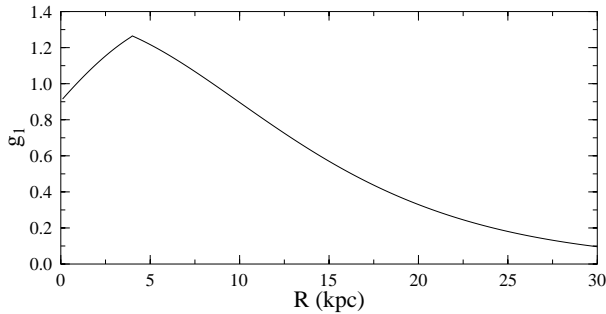


Fig. 2. This diagram shows the modelled radial distribution of the parameter $g_1(r)$ of Eq. (3). $g_1 = 1.0$ at the position of the Sun. The radial scale length is $A_1 = 15$ kpc. This function is derived from the intensity distribution of the HHM (Pietz et al. 1998a) and is consistent with the scale length of the DIG derived from pulsar dispersion measurements by Taylor & Cordes 1993.

does not appear within our model calculations. In an analysis of the LDS data (Westphalen 1997), no indication was found for a significant variation of the linewidth of the high-dispersion-velocity component as a function of the galactocentric radius. This result suggests for our analysis that, within the uncertainties of the analysed LDS data, the NHM can be well described as an isothermal gas with a constant vertical scale height.

Pietz et al. (1998a) found that the galactic X-ray halo emission across the entire galactic sky can be fitted well with a single plasma temperature of $T = (1.56 \pm 0.06) 10^6$ K (see Fig. 10 of Pietz et al. 1998a). This implies that the HHM can be considered to be isothermal on large scales. The ionised species (Sect. 3.2.3) and the NHM show the same velocity dispersion, indicating that these components must be closely related to each other.

The maximum velocity dispersion of 60 km s^{-1} , as proposed by B&C, is in remarkably good agreement with the observational results of Kalberla et al. (1998). B&C, however, derived a velocity dispersion which varies with $|z|$. Such a variation seems to question an isothermal description of an equilibrium state. We therefore tested the applicability of their approach. In modelling the HI distribution according to B&C we got however unacceptable results at all latitudes. We conclude that the data can be modelled best by assuming an isothermal state. Here we have to point out that “isothermal” denotes a constant energy density within the galactic halo. We found that each individual gaseous component can be considered as isothermal by averaging across large parts of the galactic sky, as presented in this paper.

4.3. Galactic rotation

To model the galactic HI distribution, it is necessary to account for the differential galactic rotation. We used the rotation curve of Fich et al. (1990). Our modelling suggests that the observational data are consistent with a co-rotation of the NHM and HHM with the galactic disk. Bregman (1980) predicted that the galactic rotation slows down with increasing $|z|$. Accordingly,

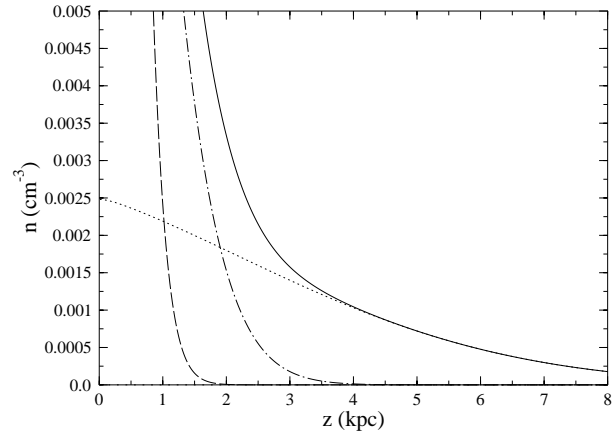


Fig. 3. Vertical density distribution for the gaseous components at the radial distance of the Sun. The dashed line marks the disk gas, the disk-halo interface is indicated by the dot-dashed line, while the dotted line represents the halo gas. The sum of all three volume densities is marked by the solid line.

the halo would be in rest at 3.6 to 6 z -scale heights, depending on R . Testing this hypothesis in fitting the HI distribution, we found that such a moderate deceleration cannot be distinguished from the situation of co-rotation. Any significantly stronger deceleration however causes problems in fitting the data.

Our finding of a co-rotating or nearly co-rotating galactic halo is also supported by the kinematical analysis of Savage et al. (1997). They found evidence that the highly ionised disk and halo gas are dynamically coupled up to distances of $|z| \simeq 5$ kpc.

5. Verification of the model

We distinguish three major regions, the galactic disk, the disk-halo interface and the galactic halo. These regions are different in their physical properties.

Based on the modelled distribution of the galactic gas components we now investigate the distribution of the magnetic fields and of the cosmic rays. To find a model which fits *simultaneously* the gas, magnetic field and cosmic ray observations, we varied $0 < \alpha < 1$ as well as $0 < \beta < 1$ individually. Unfortunately, the radio-continuum data do not allow an unambiguous separation of the magnetic field (α -term) and cosmic ray (β -term) pressure. To disentangle, at least partly, the α and β -term we studied in addition the *EGRET* data, which allow to constrain the β -term without any information about the α -term assuming that the electrons behave in the same way as the protons. The *EGRET* data contain information about the disk and disk-halo-interface, but not about the halo. This is because of the low density of the halo matter and the small cross section of the cosmic rays with the matter.

5.1. Synchrotron radiation

To derive the distribution of the magnetic fields, we analysed the 408 MHz radio continuum survey of Haslam et al. (1982). Beuermann et al. (1985) found evidence that 40% of the de-

tected 408 MHz emission of the disk is of thermal origin. Thus, we have to take a considerable contamination of the synchrotron emission in the disk into account. This emission limits the determination of α in the disk region.

In modelling the synchrotron emission at 408 MHz we followed Phillipps et al. (1981a, Sect. 3). We generalised their approach, by including the distribution of cosmic rays $n_{\text{CR}}(R, z)$ and magnetic field B explicitly. The synchrotron emission $\epsilon(l, b)$ is calculated by integrating along the line of sight s for regular $B_{\text{reg}}(R, z)$ or irregular magnetic fields $B_{\text{irr}}(R, z)$ respectively. ψ denotes the projection angle between line of sight and magnetic field vectors. We distinguish nonthermal spectral indices α_r and α_i for regular and irregular fields respectively.

$$\epsilon(l, b) = \int_0^\infty n_{\text{CR}}(R, z) \left[0.166 B_{\text{irr}}^{(1+\alpha_i)}(R, z) + 0.242 B_{\text{reg}}^{(1+\alpha_r)}(R, z) \sin^{(1+\alpha_r)} |\psi| \right] ds \quad (5)$$

It is important to take into account that the synchrotron emission from regular and irregular magnetic field components are different. Due to the $\sin^{(1+\alpha_r)} |\psi|$ term, the synchrotron emission from regions with a regular magnetic field can be distinguished from one with an irregular magnetic field structure. Using our modelled gas distribution, and a set of Parker-parameters α and β , we searched for the best fit $|z|$ -arrangement of regular and irregular magnetic fields.

It is not common to differentiate the spectral indices α_i and α_r associated with irregular and regular fields. In practice a single value of $\alpha_r = \alpha_i \simeq 0.8$ is used. However, it is a long standing discussion, whether or not the spectral index in the galactic plane differs from that of the high galactic latitudes sky. According to our model we assign different spectral indices to the irregular and regular magnetic field configuration. We use $\alpha_i = 1.0$ and $\alpha_r = 0.5$ as characteristic values for disk and halo. Here we were guided by Reich & Reich (1988) who found similar numbers for low and high latitudes from their analysis of synchrotron radiation at different wavelengths. A single non thermal spectral index $\alpha_r = \alpha_i = 0.8$ does not fit the emission close to the galactic plane as well.

Parker (1966 and 1969) discussed the coupling of magnetic fields and cosmic rays (see also Bertsch et al. 1993). In the case of an irregular magnetic field, one expects a rapid diffusion of the cosmic rays into the galactic halo (Jokipii & Parker, 1969a,b).

According to Eq. (5) the synchrotron radiation depends on both, cosmic rays n_{CR} and magnetic field B . To disclose the physical relation between these constituents we need supplementary data. We used the diffuse γ -ray emission observed with *EGRET* which will be discussed in Sect. 5.2. An additional helpful constraint was given by Parker (1969). In an equilibrium state $\alpha \leq 1$ as well as $\beta \leq 1$ is to be expected.

5.1.1. The galactic halo

Simultaneous fits to the *EGRET* γ -ray data which yield n_{CR} (Sect. 5.2) and the 408 MHz survey data give $\alpha = 1$ and $\beta = 1$

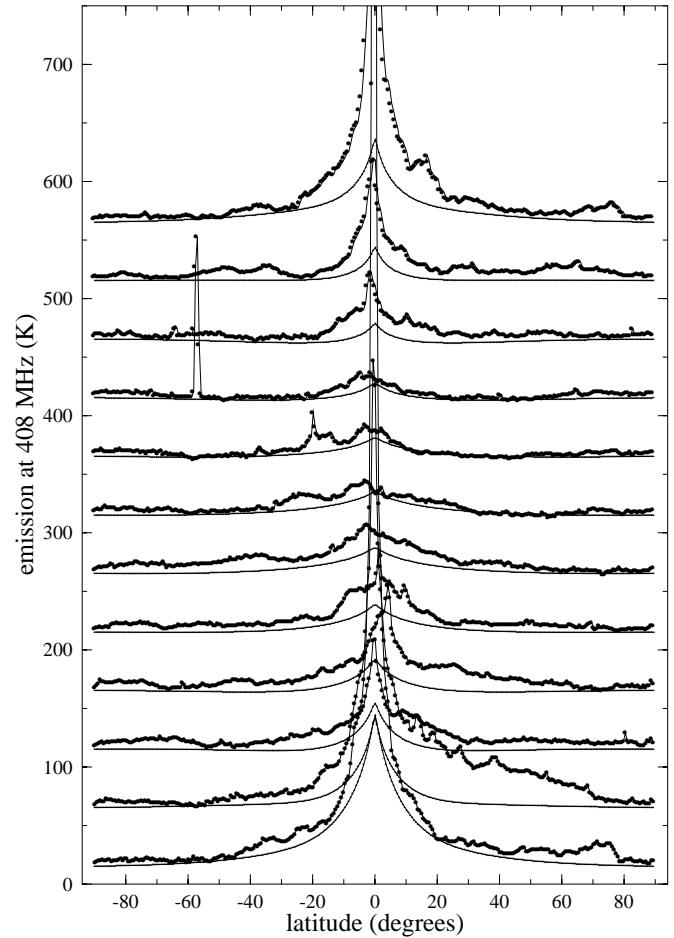


Fig. 4. The radio-synchrotron emission extracted from the 408 MHz survey of Haslam et al. (1982). Each row represents a slice in galactic latitude. The data are marked by the connected dots, while the model is represented by the solid line. The rows start at $l = 0^\circ$ (bottom) and end $l = 330^\circ$ (top) in steps of $\Delta l = 30^\circ$. The individual scans are offset by 50 K. Neither background sources nor thermal emission or emission from radio loops was eliminated from the data. Please note that only cuts in the range $180^\circ \leq l \leq 240^\circ$ are unaffected by radio loops. The model represents therefore a lower envelope to the data.

within the galactic halo. This implies a pressure equilibrium between gas, magnetic fields and cosmic rays in the halo. The magnetic field is found to be regular and oriented parallel to the galactic plane. We adopted a pitch angle of 12° determined previously by Phillipps et al. (1981a,b) and Beuermann et al. (1985).

5.1.2. The disk-halo interface

For the transition zone between galactic disk and halo we determined $\alpha = \beta = 1/3$ associated with a turbulent field. The scale height is found to be about 1 kpc. This may indicate that the DIG (Reynolds 1997) plays an important role for the disk-halo interface region with respect to the hydrostatic equilibrium considerations. These numbers indicate that the cosmic rays in the disk-halo interface are coupled to the magnetic field

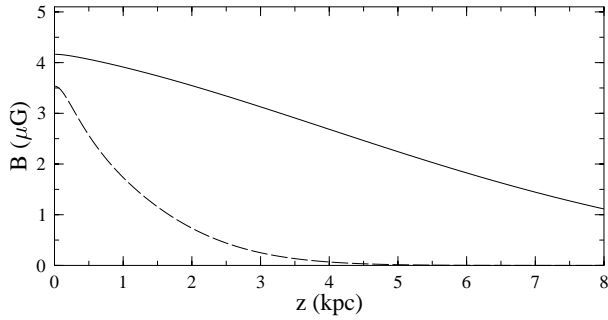


Fig. 5. Vertical distribution of the magnetic field strength in the solar vicinity. The solid line represents the magnetic field of the galactic halo which is orientated parallel to the galactic plane. The dashed line marks the magnetic field of the galactic disk, which reveals a turbulent field structure.

($\alpha = \beta = 1/3$). They are not directly coupled to the gas, otherwise we would expect $\beta = 1$.

5.1.3. The galactic disk

The synchrotron radiation close to the galactic disk was found to be fitted best assuming that the disk components are associated with completely irregular magnetic fields. Here we determined $\alpha = 1/3$ which is expected for turbulent magnetic fields in pressure equilibrium with gas (Leahy, 1991).

In the disk there is no correlation between gas and cosmic rays ($\beta=0$). This is in marked contrast to the disk-halo interface as discussed in Sect. 5.1.2.

Our findings are consistent with Hunter et al. (1997) who analysed the diffuse γ -ray emission from the galactic plane and derived a coupling scale of 1.76 kpc (HWHM). This value is consistent with our best fit one, assuming that the coupling process is isotropic. Our model gives a coupling scale of 2.07 kpc (HWHM) in z -direction for the total cosmic ray distribution derived from an equilibrium with DIG, NHM and HHM (Table 1). We tend to explain the different coupling of the cosmic rays to the disk and halo gas components by the different nature of the magnetic field in these regimes.

Fig. 4 displays the synchrotron emission observed at 408 MHz by Haslam et al. (1982) for longitudes 0° (bottom) to 330° (top), as a function of galactic latitude. Individual sources (e.g. Fornax A at $(l, b) = 240^\circ, -58^\circ$, e.g. Loop I at $l = 30^\circ$) and diffuse thermal emission have not been subtracted. Therefore, our model forms a lower envelope to the observed intensities. Fig. 4 should be compared with Phillipps et al. (1981b, Figs. 3 to 5) and Beuermann et al. (1985, Figs. 3 and 4).

The vertical distribution of the regular $B_{\text{reg}}(R_\odot, z)$ and irregular magnetic field components $B_{\text{irr}}(R_\odot, z)$ predicted by our model are shown in Fig. 5. The magnetic field in the galactic halo determines the Alfvén velocity of 180 km s^{-1} for $|z| > 4 \text{ kpc}$ (Fig. 6), indicating that the dynamical state of the galactic halo is dominated by the magnetic fields. The sound crossing timescale for the halo can be estimated to be $t_s \simeq 3 \cdot 10^8 \text{ yr}$ in radial direction (assuming a diameter of 60 kpc for the Galaxy). The

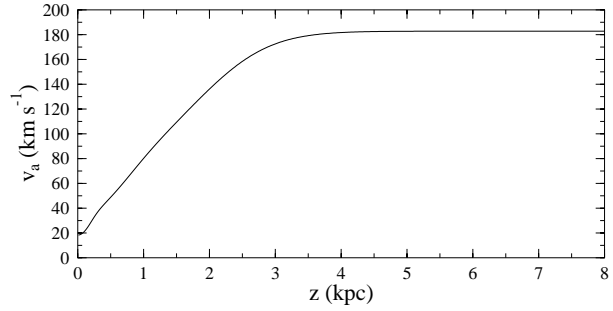


Fig. 6. Mean Alfvén velocity v_a as function of z distance to the galactic plane, derived from our model.

cooling timescale, estimated from Bregman (1980, Eq. 4.8), is comparable to this value, as is the free fall time. These numbers indicate, that on large angular scales, the galactic halo may be considered as a hydrostatic system.

5.2. γ -rays

Diffuse γ -ray emission is caused predominantly due to the nuclear interaction (π° -decay) between cosmic rays and matter (e.g. Bloemen, 1989) and inverse Compton scattering on photons. To check our results on the cosmic ray distribution, which were constrained by the synchrotron radiation at 408 MHz, we modelled the observed γ -ray intensities. We consider *EGRET* observations at energies above 100 MeV (Fichtel et al., 1994). We followed Bertsch et al. (1993) in calculating the expected count rates from nuclear and electron bremsstrahlung interactions with matter. The inverse Compton scattering data were kindly provided by A. Strong from the public “galprop” database (Strong & Moskalenko 1997). A. Strong’s Compton scattering data are calculated for a scale height of 3 kpc. Accordingly, these data are an approximation to our model, which has a scale height of 4.4 kpc, but the introduced uncertainty is negligible because it amounts to $< 5\%$.

The cosmic ray radial distribution predicted by our model is given in Fig. 7 and agrees well with the distribution derived by Webber et al. (1992, Fig. 2). The *COS-B* γ -ray emissivities (Strong et al. 1988) as a function of galactocentric radius are superimposed onto both functional dependencies.

Fig. 8 shows the *EGRET* intensities (connected dots, Fichtel et al., 1994) and our model (solid line) for longitudes 0° (bottom) to 330° (top) in steps of 30° . To improve the signal-to-noise ratio of the *EGRET* data we have averaged areas of $7^\circ \times 7^\circ$. Deviations between γ -ray observations and our model are found at low latitudes because the molecular gas phase is not included in our analyses (see Hunter et al. 1997 for further analysis of the molecular gas contribution). Fig. 8 demonstrates that the diffuse γ -ray emission at intermediate and high latitudes is well represented by our model.

Individual sources are not subtracted from the *EGRET* data. We derive a count rate of $10^{-5} \text{ s}^{-1} \text{ cm}^{-2} \text{ sr}^{-1}$ for the extragalactic background. Excess γ -ray emission is found closely correlated in position to Loop I at $l = 30^\circ$ and $0^\circ < b < 30^\circ$

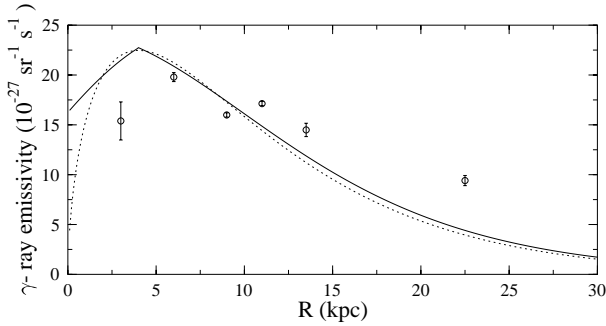


Fig. 7. The radial cosmic-ray distribution at $z = 0$ kpc predicted from our halo model (solid line). Our modelled γ -ray emissivity is in good agreement with that derived by Webber et al. (1992) within $R < 20$ kpc which is indicated by the dotted line. The data points (Strong et al., 1988, their energy independent case 2) are plotted for comparison.

as well as in the same angular range in synchrotron emission displayed in Fig. 4. Of obvious interest is also the latitude range $-40^\circ < b < 0^\circ$ at $l = 180^\circ$ (Orion). Here the enhanced gas column densities N_{H_2} , which are not included in our model, may correlate with the observed γ -ray emission.

While the synchrotron emission in the galactic halo is doubtlessly present, no significant γ -ray emission from the halo is detectable. The contribution of the galactic halo to the observed γ -ray intensities are two orders of magnitude below the *EGRET* detection limit. This is due to the small cross section combined with the low gas density in the galactic halo. On the other hand, such a weak interaction between cosmic rays and matter in the halo suggests a long life time for the cosmic rays in the halo (Parker, 1969). The disk-halo interface however, reveals diffuse γ -ray emission in intermediate latitudes which is clearly visible in Fig. 8.

5.3. Scaling relations

Throughout this paper we term scale height $H_{1/e}$ (or accordingly scale length) always in the sense of an exponential scale height defined at $1/e$ of the maximum. In the literature often “half power thickness” H_{FWHM} is used where $H_{\text{FWHM}} = 1.6 H_{1/e}$. Scales from leaky box models are usually $H_{\text{LBM}} = 0.8 H_{1/e}$ and termed “half-heights”.

In addition we need to distinguish between scale heights of physical parameters in comparison with scale heights measured from observed maps. The scale heights of our equilibrium model are defined by the gas volume densities n . Synchrotron radiation, γ -ray emission, H_α and diffuse X-ray radiation of the halo are proportional to n^2 . Except for the scale height of H I and highly ionised atoms, all others which are derived directly from observational quantities correspond to only half the relevant physical scale height.

After these remarks we compare our results with already published scales. Bloemen (1987) postulated a hot gaseous halo with a z scale height of ≥ 5 kpc, Ferrière (1995, 1996) used a scale height of 4.3 kpc to derive hot gas filling factors and to

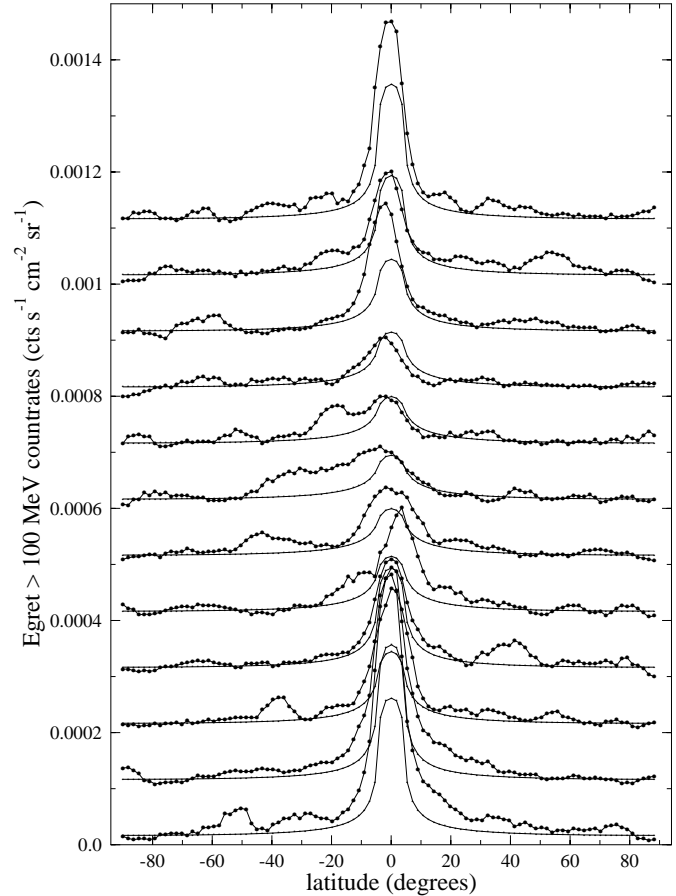


Fig. 8. The *EGRET* diffuse γ -ray emission at energies > 100 MeV (connected dots) starting at $l = 0^\circ$ (bottom) to $l = 330^\circ$ (top) in steps of $\Delta l = 30^\circ$. The data have been averaged over areas of $7^\circ \times 7^\circ$. The individual scans are offset by $10^{-4} \text{ s}^{-1} \text{ cm}^{-2} \text{ sr}^{-1}$. The solid line represents the model calculations.

estimate turbulent magnetic diffusion. Wolfire et al. (1995) proposed a two-phase neutral hydrogen medium in pressure equilibrium with a hot galactic corona of a similar scale height.

From observations, scale heights for the gaseous component between 1 kpc and 5 kpc have been derived by Lockman & Gehman (1991), Danly (1990), Savage et al. (1997) and many others. Evidence for a galactic halo extending up to a few kpc was recently reported by Dixon et al. (1998) based on γ -ray observations.

Based on the 408 MHz survey (Haslam et al., 1982) Beuermann et al. (1985) found in z direction a scale height of 1.5 kpc for the synchrotron emission in the solar vicinity. Our model predicts a scale height of 2.2 kpc. In case of a scale height of the cosmic ray distribution, of 4.4 kpc in accordance with our model, Webber et al. (1992) find an upper limit of 4.8 kpc for low cosmic ray convection velocities in the galactic halo. More recently Strong & Moskalenko (1997) derived a halo scale height of 3 kpc.

The galactocentric scale length of the gas derived by us $A_1 = 15$ kpc, yields for $\alpha = \beta = 1$ a scale length of the synchrotron radiation of 7.5 kpc, whereas Beuermann et al. (1985)

found 5.7 kpc. However, our model predicts an identical distribution for the DIG (within the errors) as determined by Taylor & Cordes (1993) or Lazio & Cordes (1998). Our predicted radial distribution of the cosmic rays (Fig. 7) is in excellent agreement with the one published by Webber et al. (1992, their Fig. 2) for galactocentric distances up to $R = 20$ kpc.

Such common radial and vertical scales suggest similar energy sources and probably also similar diffusion processes for gas and cosmic rays. From stability considerations (Sect. 6) we find that the gaseous halo has to be supported by the turbulent pressure of the disk gas. It appears reasonable to assume that super-bubbles and supernovae account for the turbulent gas pressure in the disk (Norman & Ferrara, 1996). This class of sources appears to be the origin for the galactic cosmic rays as well (Ginzburg & Syrovatskii, 1964).

6. Stability considerations

Since Parkers (1966) classical publication all halo models were faced with the major problem to fit the observational data and *simultaneously* to be consistent with a stable hydrostatic equilibrium configuration. In this section we study the stability of our disk-halo model. We follow the stability analysis of Bloemen (1987) and B&C. As discussed by these authors in detail, the generalised stability criteria of Lachièze-Rey et al. (1980) may be applied to a hydrostatic model, which demands that a vertical flux tube has to be stable. According to Bloemen (1987) stability is described by

$$\gamma p(z) > P_{\text{gmin}}(z) = -\frac{n^2(z) \partial\Phi/\partial z}{\partial n/\partial z}. \quad (6)$$

where $p(z)$ is the total gas pressure and γ the polytropic index of the gas. The polytropic indexes for gas, magnetic fields, and cosmic rays are uncertain. Concerning the gas, which is most important in this context, Parker (1966) argued for $\gamma = 1$, equivalent to the isothermal case. For the NHM, as analysed by Kalberla et al. (1998), there is evidence that the detected line widths are caused by Kolmogoroff type turbulence, supporting the assumption of an incompressible gas. In Sect. 8 this topic will be discussed in more detail. Since observations of the NHM and HHM in general fit best to an isothermal gas (as discussed in Sect. 4.1.2), we set $\gamma = 1$ for the gas, as Parker (1966) did. In Fig. 9 the minimum gas pressure required for stability $P_{\text{gmin}}(z)$ (solid line) is always less than the total gas pressure $p(z)$ (dotted line). Apparently the stability criterion given in Eq. (6) is satisfied for all z -distances.

The result of our stability analysis may be compared with Bloemen (1987) or with B&C, who attempted to derive a stable halo from the parameters of the gaseous components known at that time. From their investigations it became obvious that the conventional layers associated with the galactic disk (CNM and WNM) fail to maintain a stable halo. To gain a deeper insight, under which circumstances the halo may be protected from ‘‘Parker instabilities’’, we varied the gas parameters from those compiled in Table 1. The result is, that a stable halo needs

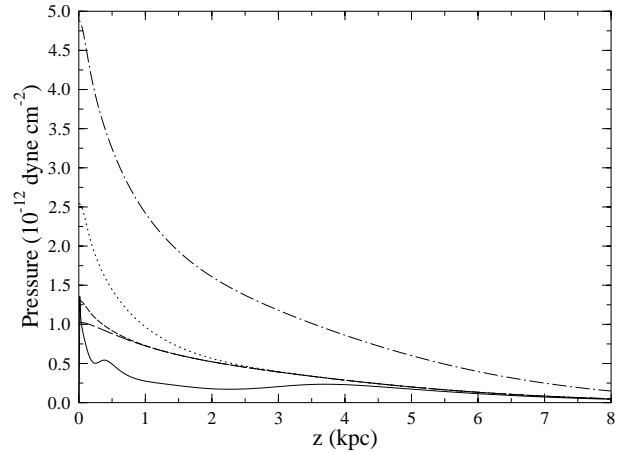


Fig. 9. Vertical pressure distribution in the solar vicinity: gas (dotted line), magnetic field (dashed line) and cosmic rays (long dashed line) sums to the total pressure (dash-dot line). The solid line represents the minimum gas pressure required for stable hydrostatic equilibrium of the galactic halo. The modelled galactic halo is stable on average. Local instabilities may occur only beyond a vertical distance limit of 4 kpc.

pressure support from the galactic plane. A hierarchical multicomponent disk-halo composition is required, according to Avillez (1997) built up by a galactic fountain flow. In case of a single gaseous component no stable solution can be found, consistent with Parker’s (1966) analysis.

The DIG is of most importance here. It is the disk-halo interface which accounts dominantly for the stability of the halo. Though, the scale height of the DIG is 0.95 kpc only, its high pressure stabilises the matter within the galactic halo up to z distances of 4 kpc. This is because of its high mid plane density, which is an order of magnitude larger than that of the halo gas (HHM & NHM). The DIG has to be distinguished from the disk for an additional reason: The DIG is located intermediate between the disk and halo, accordingly it couples the cosmic rays to the magnetic field in between. Here it appears worth to have a look at Fig. 6: while the Alfvén velocity is constant above $|z| \gtrsim 4$ kpc, a continuous velocity decrease is predicted by our model with decreasing vertical distance from the galactic plane. Obviously the DIG is interfacing disk and halo.

One has to be careful, however, because Eq. (6) is necessary for stability, but may not be sufficient. (See Lachièze-Rey et al. (1980), Bloemen (1989) and B&C for detailed discussion). Fig. 9 gives the *average* pressures only. Local fluctuations of the pressure or temperature variation may cause local ‘‘Parker instabilities’’. Being conservative, we take for sure only that the galactic halo is stable up to z distances of ~ 4 kpc. Regions above this limit may be affected by instabilities. Our simulations indicate, that instabilities will occur if the gas pressure of the HHM increases significantly. The scaleheight of the HHM may not exceed 6 kpc. Instabilities will occur also if either the temperature of the HHM drops below $T \simeq 10^6$ K or if the average density of the NHM component exceeds that of the HHM significantly.

HVCs may have their origin at $|z| \gtrsim 4$ kpc, a hypothesis which is frequently suggested in galactic fountain models (e.g. Bregman 1980). This is also consistent with our model, because at such z distances thermal instabilities can probably trigger the cloud condensation. Our distance estimates of $|z| \gtrsim 4$ kpc are in good agreement with recently determined distance limits of some HVC complexes (Wakker & van Woerden 1997). Van Woerden et al. (1998) present evidence that complex A has a distance of $3 \text{ kpc} < |z| < 7 \text{ kpc}$ from the galactic plane. Assuming that the condensations observed in complex A are in equilibrium with the total pressure represented in Fig. 9 we estimate a distance $z \simeq 3.6$ kpc for these HVC clumps.

If HVCs originate from instabilities, as suggested above, one should find a correlation between HVC complexes and parameters of the gaseous halo. Indeed, a general correlation of HVC complexes C, A and GCN with enhanced diffuse X-ray radiation at 1/4 keV was claimed by Kerp et al. (1996, 1998) and Pietz et al. (1998a,b). Such an excess X-ray emission may be interpreted as an indication of enhanced cooling in the vicinity of the HVC complexes. From our model we can estimate an upper limit for z distances. Galactic HVCs can be formed if they condensate out of halo matter in a global hydrostatic equilibrium. Above $|z| \simeq 10$ kpc less than 1% of the gaseous halo mass is available. Thus a significant amount of HVCs can originate from such regions only if the gas was ejected to such heights in a non-equilibrium event, such as a galactic fountain.

So far we discussed the stability perpendicular to the galactic disk. Radial stability demands for a flat rotation curve a velocity dispersion of the gas of $\sigma \gtrsim 220/\sqrt{8} \simeq 78 \text{ km s}^{-1}$ (Pfenniger et al. 1994). The observed dispersion in direction to the north galactic pole is $\sigma = 60 \pm 3 \text{ km s}^{-1}$. From the Kolmogoroff relation we derive a dispersion of $\sigma = 76 \pm 4 \text{ km s}^{-1}$ across the total disk. The observed turbulent motions are isotropic, we conclude therefore that the halo gas can stabilize the galactic disk in radial direction, provided however that this gas is associated with a massive component.

7. The gaseous halo - a tracer of dark matter?

For a galaxy in hydrostatic equilibrium, the 3-D distributions of gas pressure, density and gravitational potential are identical in shape. Buote & Canizares (1996) suggest that shapes and sizes of elliptical galaxy halos can be derived from X-ray observations. We applied this theorem to the Milky Way using the distribution of the HHM according to Pietz et al. (1998a).

We assume a mass model for the Galaxy based on three constituents: a galactic bulge, a stellar disk with a radial scale length of $\simeq 4.5$ kpc and gas with a scale length of $\simeq 15$ kpc. Assuming that the gaseous halo traces the dark matter distribution we simply need to scale the density of the observed gaseous halo until the rotation curve for the model distribution is in agreement with the observed rotation velocities. As best fit values we derive in the solar vicinity a surface density of $\simeq 37 M_{\odot} \text{ pc}^{-2}$ for the stellar disk and a total surface density of $\simeq 141 M_{\odot} \text{ pc}^{-2}$ for the gas including the halo.

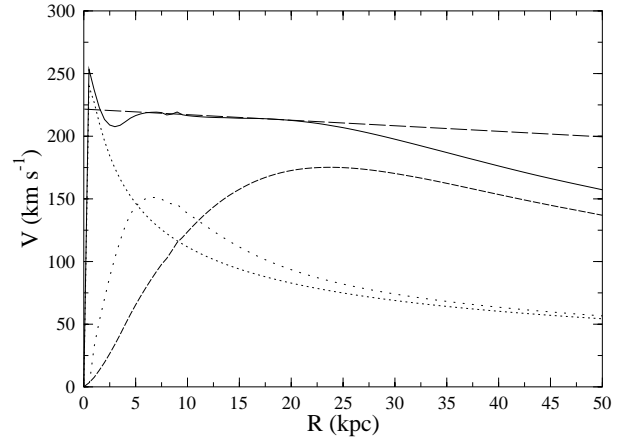


Fig. 10. The galactic rotation curve, assuming that the gaseous halo phase traces the dark matter content, is represented by the solid line. The contribution of the gas including the massive halo (short dashed line), the stellar disk and bulge (dotted lines) according to the model are plotted. For comparison, the linear approximation of the galactic rotation curve according to Fich et al. (1990) is given (long dashed line). For $R \lesssim 12$ kpc the stellar component determines the rotation, at larger radii the gas.

Fig. 10 shows the corresponding rotation curve. In comparison with the rotation curve from Fich et al. (1990) we find acceptable agreement within galactocentric radii $3 < R < 25$ kpc. The total mass of the Galaxy derived this way is $M = 2.8^{(+1.0)}_{(-0.5)} 10^{11} M_{\odot}$, in agreement with $M = 2.4 10^{11} M_{\odot}$ derived by Little & Tremaine (1987) and also, within the uncertainties, consistent with the results of Kochanek (1996) of $M = 4.9 10^{11} M_{\odot}$. The halo mass is $M_{halo} \simeq 2.1 10^{11} M_{\odot}$. The equivalent midplane density of the dark matter in the solar vicinity derived from such an assumption amounts to $n_{DM} \simeq 0.72 \text{ cm}^{-3}$, about 300 times the density of the gaseous halo constituents we have used in our model (NHM & HHM).

8. Turbulence

von Weizsäcker (1951) first pointed out that turbulence in the interstellar medium can be studied by comparing the observed linewidths σ (denoted here as the velocity dispersions) with the linear sizes l of the emitting regions. According to Fleck (1983) turbulent motions can be described by a power law $\sigma(l) \sim l^{\nu}$. The well known Kolmogoroff relation with $\nu = 1/3$ is valid for an incompressible medium only.

The boundary conditions for $\nu = 1/3$ are rather stringent: the turbulent energy of the overall flow must be transmitted without dissipation from the largest to the smallest eddies. Viscous dissipation is permitted only on the small scale end of this cascade. As pointed out by Fleck (1983), a significant fraction of the gaseous disk is in supersonic motion. Shocks and cloud-cloud collisions must occur, causing energy dissipation on intermediate scales. For a compressible medium $\nu > 1/3$ is expected.

Our model is based on the assumption that the gaseous halo is isothermal. In Sect. 6 we assumed that a polytropic index $\gamma = 1$, belonging to an incompressible medium, can be assigned

to the gaseous halo. Then the turbulent flow in the galactic halo can be described by the Kolmogoroff relation with $\nu = 1/3$.

Kalberla et al. (1998, see their Fig. 3) found that on average the NHM line widths increase with path lengths according to the Kolmogoroff relation. This result applies to scale lengths between 4.4 kpc and 10 kpc.

Here we try to determine the smallest scale at which the turbulent flow has to terminate. We assume that any turbulent energy transfer becomes irrelevant when the energy density of the turbulent flow is comparable to the energy density of the cosmic microwave background. At a temperature of 3 K the turbulent line width of H I gas is $\sigma = 0.15 \text{ km s}^{-1}$ and from the Kolmogoroff relation we obtain the minimum turbulent scale length of $l_{min} \sim 20 \text{ au}$. This is a lower limit since dissipative processes must increase the index ν (Fleck, 1983).

“Tiny-scale atomic structure” (see Heiles 1997) was observed at scales of several tens of au, down to $\sim 25 \text{ au}$. Walker & Wardle (1998) suggested that gaseous clumps with radii of $\lesssim 20 \text{ au}$ may be responsible for extreme scattering events. They propose that a large fraction of the dark matter may be in this form. Pfenninger & Combes (1994) argue that cold gas clouds with radii of $\gtrsim 30 \text{ au}$ must exist in the outer disk. Assuming that the total halo mass is associated with fractal structure, we estimate from Eq. (5) of Pfenninger & Combes (1994), that the mass of such a 20 au cloud is $M_{clump} \lesssim 2 \cdot 10^{-3} M_{\odot}$. Such clumps (and similar massive objects) contribute to the gravitational potential but not to the gas pressure according to Eq. (1). We demonstrated in Sect. 7 that the gaseous halo components (NHM and HHM) can be interpreted as tracers of dark matter in the halo. Considering the turbulent properties of the halo gas (NHM and highly ionised atoms), we infer that the observable H I lines may be regarded as tips of cold and massive “icebergs”.

The conclusions drawn in this section depend strongly on the assumption, that the gaseous halo can be treated as an incompressible gas. To study the question whether it is possible to have a turbulent flow without dissipative events, we first estimate the filling factor for the NHM. This H I gas is interspersed in a plasma. Assuming that the NHM is locally in pressure equilibrium with the HHM we derive a volume filling factor of 0.12 for the NHM, consistent with Ferrière (1995). This implies that the distance between H I eddies is twice as large as their diameter. Next we consider the motion of such an H I eddy with respect to the surrounding plasma. Comparing the observed turbulent speed of 60 km s^{-1} in the halo with the Alfvén speed or isothermal sound speed for the HHM, we find that the motion of the H I eddies within the plasma is *subsonic* on all scales. We conclude that within a *multiphase* medium, as presented here, dissipative events due to shocks or cloud-cloud collisions are of little relevance.

9. Summary and discussion

We use a hydrostatic halo model, as proposed by Parker (1966), to analyse the large scale distribution of gas, magnetic fields and cosmic rays in the Galaxy. Parker’s approach was based on the assumption that the interstellar magnetic field, gas and

cosmic rays form a system in dynamical equilibrium with the gravitational potential. According to Parker’s considerations, the gas must be fully interwoven with the magnetic field. The gas density cannot be too low, otherwise magnetic field and cosmic rays would expand outward from the disk and be lost.

Since the early fifties it is known from optical polarisation studies that the Galaxy must have an interstellar magnetic field with a field strength of a few μG , which is, on the average, oriented parallel to the galactic disk. Moreover, there is clear evidence for radio synchrotron emission originating at distances of a few kpc above the galactic plane. Thus, magnetic fields and cosmic rays are constituents of the galactic halo. Until now there was no unique evidence for an associated gas phase.

Since 1966, a number of attempts have been made to explain the nature of the galactic halo, none of them is entirely convincing. Either the models were found inconsistent with the observational data, or they predicted an unstable galactic halo.

Recent investigations of the *ROSAT* soft X-ray background gave evidence for the existence of a plasma with temperatures of $T \simeq 1.5 \cdot 10^6 \text{ K}$. The galactic halo plasma has a vertical scale height of about 4.4 kpc (Pietz et al. (1998a). At such heights also highly ionised atoms have been observed (Savage et al. 1997).

Last but not least, sensitive H I data gave evidence that neutral atomic hydrogen is present at such z distances too, with turbulent velocities well comparable to those of the highly ionised gases ($\sigma \simeq 60 \text{ km s}^{-1}$, Kalberla et al. (1998) and Savage et al. (1997)). There is evidence that the highly ionised gas as well as the H I gas at high z distances co-rotate with the galactic disk.

All these findings suggest first, the existence of an ubiquitous gas phase within the galactic halo and second, that the halo plasma, the highly ionised gas, and the halo H I gas are all distributed in a similar way. The comparison of the observationally derived scale height of 4.4 kpc with the observed turbulent velocities of $\simeq 60 \text{ km s}^{-1}$ (NHM and absorption line measurements of Savage et al. 1997) indicates, that the turbulent gas pressure is not high enough to support the gas at this large z distance above the galactic plane. The gas pressure has to be increased by a factor of $\simeq 3$. This factor of 3 was already introduced by Parker’s “classical” halo model, if gas, magnetic fields and cosmic rays are in pressure equilibrium. The fact, that the observed scale height of the galactic synchrotron emission is close to that expected for a gaseous phase in pressure equilibrium with magnetic fields and cosmic rays provides a further indication in favour of such a quasi equilibrium state. In this paper we studied this situation in detail.

We found a self-consistent model with three distinctly different regimes:

1. The galactic disk with scale heights of $\simeq 0.4 \text{ kpc}$ is dominated by its high gas pressure. The associated magnetic field is turbulent, its pressure only $\alpha = 1/3$ of that of the gas pressure. There is apparently no cosmic ray component coupled to the gaseous disk ($\beta = 0$). Most probably the turbulent magnetic field in the disk leads to a rapid diffusion of the cosmic rays into the halo (Jokipii & Parker 1969a,b). The derived parameter $\alpha = 1/3$ for the disk was determined from

the observed synchrotron radiation close to the disk. The data can be fitted only, in agreement with Parker's model, in case of assuming that a turbulent magnetic field is associated with the gaseous components. For a turbulent magnetic field $\alpha = 1/3$ is expected (Leahy 1991). By fitting simultaneously the synchrotron emission and the γ -ray emission, we conclude that $\beta = 0$. This is in good agreement with a coupling scale of 1.7 kpc (HWHM) between the distributions of gas and cosmic rays derived by Hunter et al. (1997) which excludes a direct coupling between cosmic rays and gas on small scales in the disk.

2. In the galactic halo the magnetic field is ordered in a regular way and oriented parallel to the galactic plane. Gas, magnetic fields and cosmic rays are in pressure equilibrium, as suggested by Parker (1966), $\alpha = \beta = 1$. The gaseous halo is composed of different phases, ranging from neutral gas (H I) to plasma $T \simeq 1.5 \cdot 10^6$ K. The plasma component as well as the H I gas in the halo appear to be isothermal. On large scales we found no indication for a varying plasma temperature or velocity dispersion with varying galactic position. The scale heights are identical for the NHM and HHM. Thus, neutral gas and halo plasma seem to be intermixed on linear scales of a few kpc. The turbulent velocity dispersions for neutral and highly ionised gas are within the uncertainties identical, suggesting that the highly ionised gases share the turbulent state of the NHM (Kalberla et al. 1998 and Savage et al. 1997). One may conclude from such a close relation that the highly ionised species are located in transition layers between neutral phase and hot plasma in the halo.
3. The disk-halo interface has physical properties which were found in former works to match both, the disk and the halo. The magnetic field is turbulent ($\alpha = 1/3$) but there is evidence that the cosmic rays are coupled to the magnetic field in this range ($\beta = 1/3$). These properties become evident from our model fits. For the coupling scales between cosmic rays and gas we found within the uncertainties the same values as Hunter et al. (1997).

From Parker's (1966) investigations, it became evident that any halo model must be critically reviewed concerning its stability. We use criteria proposed by Lachièze-Rey et al. (1980) and derive that the halo is, on the average, stable. Instabilities due to fluctuations of pressure or temperature may arise at $|z| \gtrsim 4$ kpc. We conclude that HVCs, which have been suggested to condense in the galactic halo (Bregman 1980), may originate from regions above $|z| \gtrsim 4$ kpc.

The outstanding properties of the disk-halo interface become obvious when analysing the stability of the halo. Simulating the stability of a disk-halo system under various conditions, we realize that the properties of the DIG are most important for the stability of the lower halo. Evidently, the disk-halo interface supports the halo. Within the disk-halo interface the turbulent galactic magnetic field is transformed into the regular magnetic field structure associated with the galactic halo.

Buote & Canizares (1996) have shown that shapes and sizes of galactic halos can be derived from the shapes of their X-ray halos. Assuming that the observed gaseous halo components trace the dark matter distribution accordingly leads to a flat rotation curve and a total mass of $M = 2.8^{(+1.0)}_{(-0.5)} 10^{11} M_{\odot}$ for the Milky Way.

Turbulence in the galactic halo probably follows the Kolmogoroff relation. The smallest clouds which are consistent with a dissipationless turbulent flow in the halo can have linear sizes of ~ 20 au and masses of $\lesssim 2 \cdot 10^{-3} M_{\odot}$. As proposed by Pfenniger & Combes (1994) a significant fraction of the halo matter may be in this form. The observed H I lines with velocity dispersions of $\sigma \simeq 60$ km s $^{-1}$ must then be regarded as tips of massive "icebergs".

In his review on theories of the hot interstellar gas Spitzer (1990) criticised halo models with the words: "With so many uncertainties involved, a hydrostatic equilibrium model can readily be made consistent with the data." Our approach was based on recent *observational* evidence for a gaseous halo, most important the halo plasma phase, but also the H I and the highly ionised gases which allowed to define a common scale height as well as a common dynamical state. Important, with respect to Spitzer's remark, is also the observational determination of the coupling between cosmic rays and gas. From a large number of model calculations, we found a self-consistent solution, which turned out to be stable at the same time. We cannot give a general proof that our model is unambiguous; however, given the internal consistency of the recent analyses of the gaseous halo components, we are confident that our approach can stand Spitzer's premonitions.

Acknowledgements. J. Kerp thanks the Deutsche Forschungsgemeinschaft for support under the grant No. ME 745/17-2. We are grateful to A. Strong for providing his "galprop" database. We thank J. Lockman, W. Hirth, U. Mebold, K.S. de Boer, R.J. Dettmar, Y. Shchekinov, H.J. Fahr and especially J. Pietz for various helpful comments and discussions, E.M. Berkhuijsen for her very constructive criticism and the anonymous referee for comments which were very helpful to improve the quality of the paper.

References

- Avillez M.A., 1997, Ph.D thesis, University of Évora.
 Bertsch D.L., Dame T.M., Fichtel C.E., et al., 1993, ApJ 416, 587.
 Beuermann K., Kanbach G., Berkhuijsen E.M., 1985, A&A 153, 17.
 Bienaymé O., Robin A.C., Crézé M., 1987, A&A 180, 94.
 Bloemen J.B.G.M., 1987, ApJ 322, 694.
 Bloemen J.B.G.M., 1989, ARA&A 27, 469.
 de Boer H., 1990, IAU Symp. 144, "The interstellar disk halo connection in Galaxies", ed. H. Bloemen, Kluwer, 333.
 Boulares A., Cox D.P., 1990, ApJ 365, 544 (B&C).
 Bregman J.N., 1980, ApJ 236, 577.
 Buote D.A., Canizares C.R., 1996, ApJ 457, 565.
 Burton W.B., 1988 in "Galactic and Extragalactic Radio Astronomy", eds. Verschuur G.L., Kellermann K.I., 295.
 Crézé M., 1991, IAU Symp. 144, "The interstellar disk halo connection in Galaxies", ed. H. Bloemen, Kluwer, 313.
 Danly L., 1990, IAU Symp. 144, "The interstellar disk halo connection in Galaxies", ed. H. Bloemen, Kluwer, 53.

- Dickey J.M., Lockman F.J., 1990, *ARA&A*, 28, 215.
- Dixon D.D., Hartmann D.H., Kolaczyk E.D., et al., 1998, *astro-ph/9803237*.
- Ferrière K. 1995, *ApJ* 441, 281.
- Ferrière K. 1996, *A&A* 310, 438.
- Ferrière K. 1998, *ApJ* 497, 759.
- Fich M., Blitz L., Stark A.A., 1990, *ApJ* 342, 272.
- Fichtel C.E., Bertsch D.L., Chiang, J., et al., 1994, *ApJS* 94, 551.
- Fleck R.C., 1983, *ApJ* 272, L45.
- Ginzburg V.L., Syrovatskii S.I., 1964, "The Origin of Cosmic Rays", New York, Pergamon.
- Hartmann Dap, 1994, Ph.D. thesis, University of Leiden.
- Hartmann Dap, Burton W.B. 1997, "Atlas of Galactic Neutral Hydrogen", Cambridge University Press.
- Hartmann Dap, Magnani L., Thaddeus P., 1998, *ApJ* 492, 205.
- Hasinger G., Burg R., Giacconi R., et al., 1998, *A&A* 329, 482.
- Haslam C.G., Stoffel H., Salter C.J., Wilson W.E., 1982, *A&AS* 47, 1.
- Heiles C., 1997, *ApJ* 481, 193.
- Hunter S.D., Bertsch D.L., Catelli J.R., et al., 1997, *ApJ* 481, 205.
- Jokipii J.R., Parker E.N., 1969a, *ApJ* 155, 777.
- Jokipii J.R., Parker E.N., 1969b, *ApJ* 155, 799.
- Kalberla P.M.W., Westphalen G., Mebold U., Hartmann Dap, Burton W.B., 1997a, in Proc. of 156. WE-Heraeus-Seminar on "The Physics of Galactic Halos", eds. H. Lesch, R.-J. Dettmar, U. Mebold, & R. Schlickeiser, Akademie Verlag, Berlin, 3.
- Kalberla P.M.W., Westphalen G., Mebold U., Hartmann Dap, Burton W.B., 1997b, in Proceedings of the IAU Colloquium No. 166 "The Local Bubble and Beyond", eds. D. Breitschwerdt, M.J. Freyberg, J. Trümper, Lecture Notes in Physics 506, 475.
- Kalberla P.M.W., Westphalen G., Mebold U., Hartmann Dap., Burton W.B., 1998, *A&A* 332, L61.
- Kerp J., Mack K.-H., Egger R., et al., 1996, *A&A* 312, 67.
- Kerp J., Burton W.B., Egger R., et al., 1998, *A&A*, submitted.
- Kochanek C.S., 1996, *ApJ* 457, 228.
- Kuijken K., Gilmore G., 1989, *MNRAS* 239, 605.
- Kulkarni S.R., Fich M., 1985, *ApJ* 289, 792.
- Lachize-Rey M., Asséo E., Cesarsky C.J., Pellat R., 1980, *ApJ* 238, 175.
- Lazio T.J.W., Cordes, J.M., 1998, *ApJ* 497, 238.
- Leahy J.P., 1991, in "Beams and Jets in Astrophysics", ed. P.A. Hughes, Cambridge University Press, 100.
- Little B., Tremaine S., 1987, *ApJ* 320, 493.
- Lockman F.J., Gehman C.S., 1991, *ApJ* 382, 182.
- Münch G., Zirin H., 1961, *ApJ* 133, 11.
- Norman C.A., Ferrara A., 1996, *ApJ* 467, 291.
- Parker E.N., 1966, *ApJ* 145, 811.
- Parker E.N., 1969, *Space Sci. Rev.* 9, 654.
- Pfenniger D., Combes F., Martinet L., 1994, *A&A* 285, 79.
- Pfenniger D., Combes F., 1994, *A&A* 285, 94.
- Phillipps S., Kearsy S., Osborne J.L., Haslam C.G.T., Stoffel H., 1981a, *A&A* 98, 286.
- Phillipps S., Kearsy S., Osborne J.L., Haslam C.G.T., Stoffel H., 1981b, *A&A* 103, 405.
- Pietz J., Kerp J., Kalberla P.M.W., et al., 1998a, *A&A* 332, 55.
- Pietz J., Kerp J., Kalberla P.M.W., et al., 1998b, in Proceedings of the IAU Colloquium No. 166 "The Local Bubble and Beyond", eds. D. Breitschwerdt, M.J. Freyberg, J. Trümper, Lecture Notes in Physics 506, 471.
- Pikelner S.B., Shklovsky I.S., 1958, *IAU Symposium* 8, Reviews of Modern Physics, 30, 935.
- Reich W., Reich P., 1988 *A&A* 196, 211.
- Reynolds R.J. 1997, in Proc. of 156. WE-Heraeus-Seminar on "The Physics of Galactic Halos", eds. H. Lesch, R.-J. Dettmar, U. Mebold, & R. Schlickeiser, Akademie Verlag, Berlin, 57.
- Savage B.D., Sembach K.R., Lu L., 1997, *AJ* 113, 2158.
- Snowden S.L., Cox D.P., McCammon D., Sanders W.T., 1990, *ApJ* 354, 211.
- Snowden S.L., Mebold U., Hirth W., Herbstmeier U., Schmitt J.H.M.M., 1991, *Sci* 252, 1529.
- Snowden S.L., Freyberg M.J., Plucinsky P.P., et al., 1995, *ApJ* 454, 643.
- Snowden S.L., Egger R., Finkbeiner D.P., Freyberg M.J., Plucinsky P.P. 1998, *ApJ* 493, 715.
- Spitzer L. 1956, *ApJ* 124, 20.
- Spitzer L. 1942, *ApJ* 95, 329.
- Spitzer L. 1990, *ARA&A* 28, 71.
- Stark A.A., Gammie C.F., Wilson R.W., et al., 1992, *ApJS* 79, 77.
- Strong A.W., Bloemen J.B.G.M., Dame T.M., et al., 1988, *A&A* 207, 1.
- Strong A.W., Mattox J.R., 1996, *A&A* 308, L21.
- Strong A.W., Moskalenko I.V., 1997, in Proc. 4th Compton Symposium AIP 410, 1162.
- Taylor J.H., Cordes J.M., 1993, *ApJ* 411, 674.
- Wakker B.P., van Woerden H., 1997, *ARA&A* 35, 217.
- Walker M., Wardle M., 1998, *ApJ* 498, L125.
- Wang Q.D., 1998, in Proceedings of the IAU Colloquium No. 166 "The Local Bubble and Beyond", eds. D. Breitschwerdt, M.J. Freyberg, J. Trümper, Lecture Notes in Physics 506, 503.
- Webber W.R., Lee M.A., Gupta, M., 1992, *ApJ* 390, 96.
- von Weizsäcker C.F., 1951, *ApJ* 114, 165.
- Westphalen G., 1997, Ph.D. thesis, University Bonn.
- Westphalen G., Kalberla P.M.W., Mebold U., Hartmann Dap, Burton W.B., 1997, in Proc. of 156. WE-Heraeus-Seminar on "The Physics of Galactic Halos", eds. H. Lesch, R.-J. Dettmar, U. Mebold, & R. Schlickeiser, Akademie Verlag, Berlin, 27.
- van Woerden H., Wakker B., Schwarz U.J., Peletier R.F., Kalberla P.M.W., 1998, in Proceedings of the IAU Colloquium No. 166 "The Local Bubble and Beyond", eds. D. Breitschwerdt, M.J. Freyberg, J. Trümper, Lecture Notes in Physics 506, 467.
- Wolfire M.G., McKee C.F., Hollenbach D., Tielens A.G.G.M., 1995, *ApJ* 453, 673.